CHAPTER IV

RESULTS AND DISCUSSION

4.1 Investigation of the Synthesis Methods of W-MCM-41

4.1.1 Formation of W-MCM-41 in Acidic Condition

With an attempt in synthesizing W-MCM-41 in acidic condition as claimed by Zhang *et al.*[50], the method was found unrepeatable. Only amorphous phase was obtained and its XRD pattern was shown in Figure 4.1a. There is no characteristic peak of the MCM-41 structure. This is in agreement with Ookawa *et al.*[65] that the mesophase of MCM-41 is not stable in acidic condition.

4.1.2 Formation of W-MCM-41 in an Basic Condition

With an attempt in basic condition as reported by Cho *et al.*[63], it in turn yields a very nice product of MCM-41 structure as proven by the XRD pattern in Figure 4.1b. The XRD of the tungsten-containing MCM-41 exhibits the typical hexagonal lattice corresponding to four characteristic peaks of MCM-41, i.e. (100), (110), (200), and (300) lattice planes from left to right, respectively. This has been suggested that the MCM-41 structure is more stable in basic condition although it was claimed that incorporation of tungsten in the MCM-41structure is preferential in acidic condition. The ICP analysis indicates that quite small amount of tungsten

was found in the product. Using the gel with Si/W of 100 results in the MCM-41 with the Si/W of 1600. Therefore, it is very challenging to practice for the direct method of synthesizing W-MCM-41 in basic condition with higher tungsten content.

Considering the XRD pattern shown in Figure 4.1b the intensity of the parent peak is quite sharp. Thus it may be due to the very small amount of tungsten incorporated so that makes it highly disperse in the MCM-41 structure and does not affect the order of the structure and/or due to the tungsten source itself. The latter means the solubility of ammonium tungstate is not as readily as sodium tungstate. However, it was reported that the presence of sodium reduces the incorporation of metal in the MCM-41 structure.[65] Both effects have also been studied in this work.

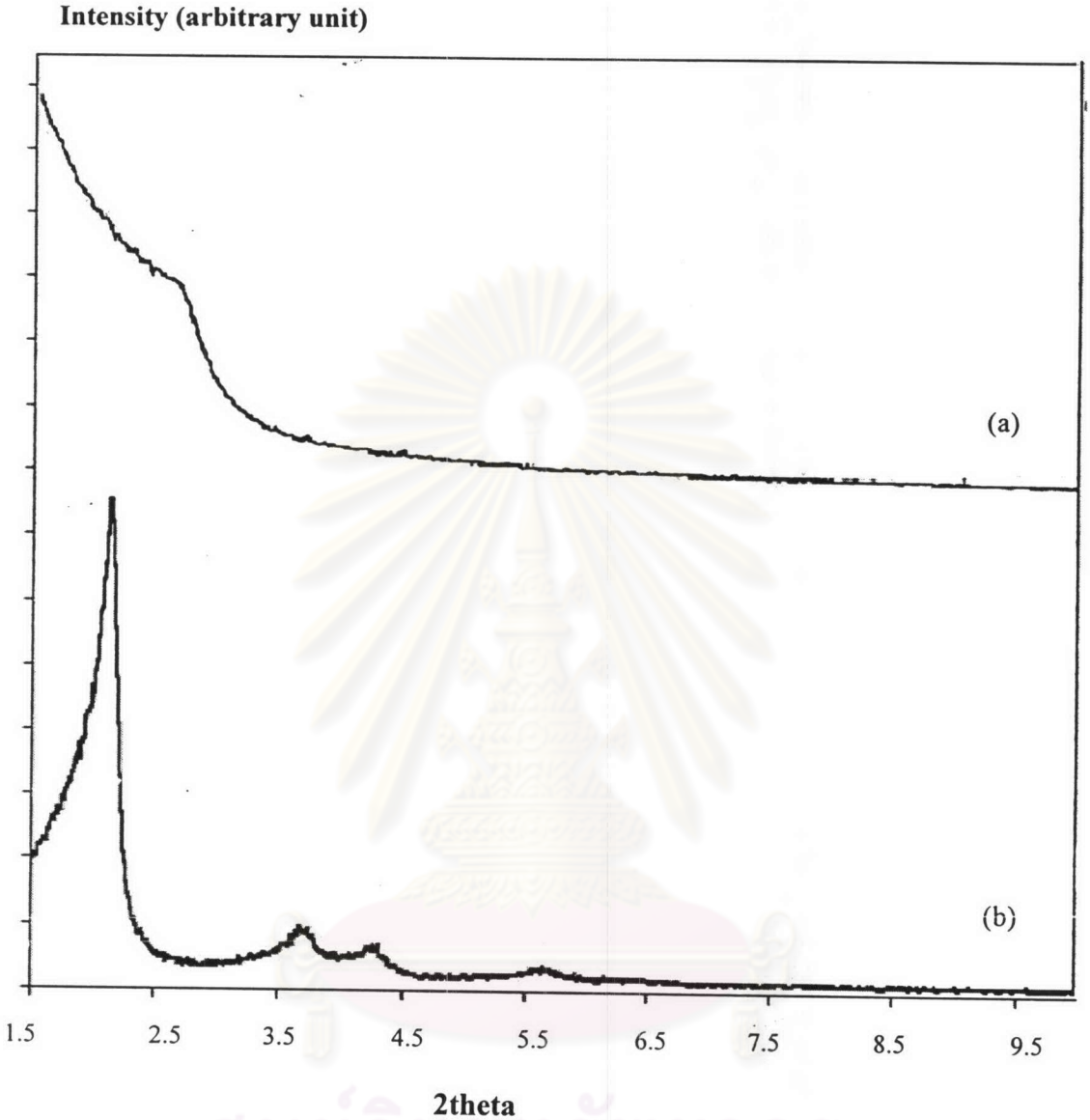

Figure 4.1 XRD patterns of as-synthesized W-MCM-41 with the Si/W ratio in gel of 100 (a) in acidic condition (b) in basic condition.

4.1.3 Effect of Tungsten Sources on Formation of W-MCM-41

W-MCM-41 samples with the same Si/W ratio in gel of 100 were synthesized in basic condition using the similar gel composition but varying the tungsten source from ammonium tungstate to sodium tungstate. The XRD patterns of both samples are shown in Figure 4.2. Assuming the same product of W-MCM-41 was obtained from both sources, the NH_4^+ and Na^+ cations must have some influence on the regularity of the MCM-41 structure due to a shift of the peak position and a change of intensity of the corresponding reflection peaks. It can be mentioned that both tungsten sources can interact with the wall of MCM-41 in the formation step of the mesophase. The interaction affects the wall thickness of MCM-41 and results in the shift of Bragg's angle (2θ) to a lower value. Ammonium tungstate is thus more appropriate than sodium tungstate due to the former provides higher ordered structure considered from higher intensity of the peak (100). Ookawa *et al.*[65] reported that tungsten from ammonium metatungstate could be incorporated into the final product more than that from sodium tungstate. However, the incorporated amount neglected. Therefore, the further study of this research favors the ammonium source from ammonium tungstate and basic condition for synthesis of W-MCM-41.

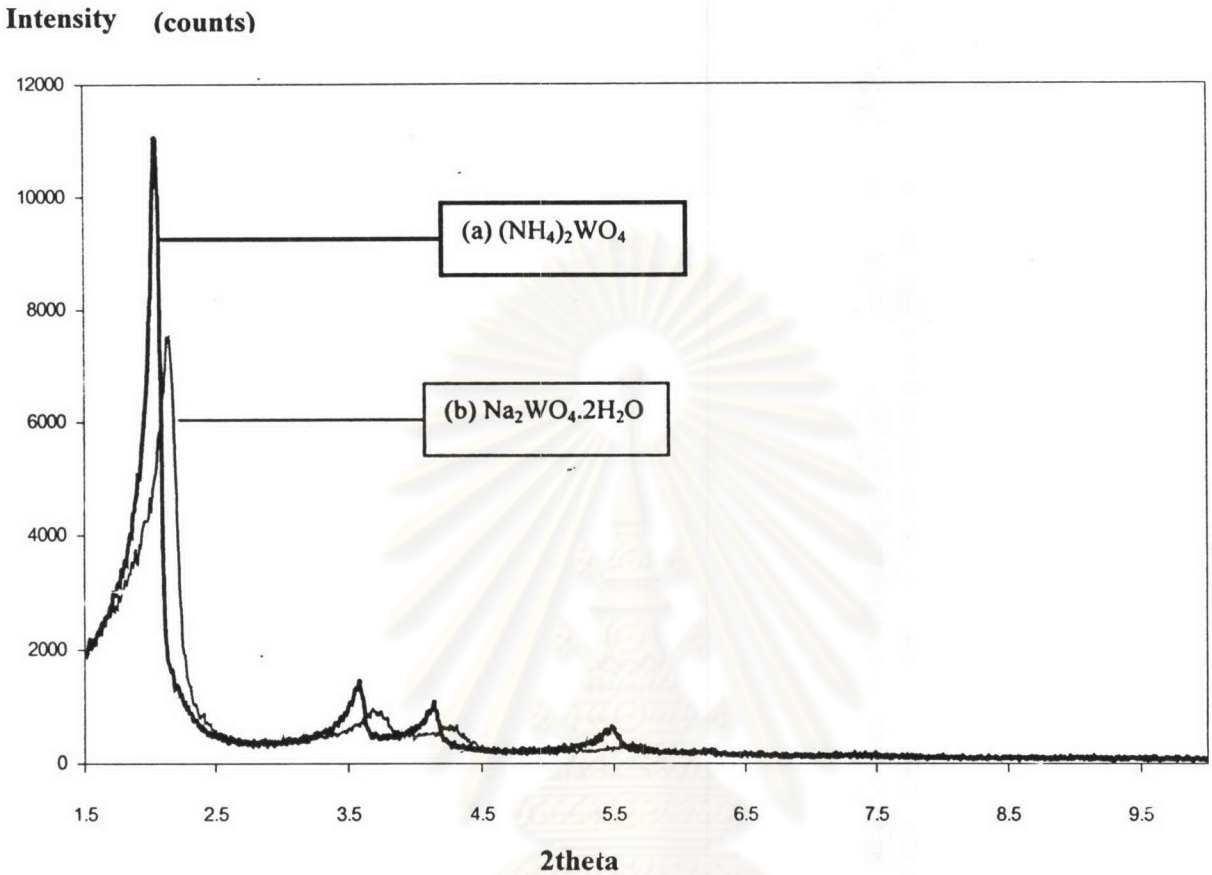

Figure 4.2 XRD patterns of as-synthesized W-MCM-41 using ammonium tungstate (a), and sodium tungstate (b), as the tungsten source.

4.1.4 Effect of the Si/W Ratios in Gel on Formation of W-MCM-41

(a) XRD results

XRD patterns of W-MCM-41 with different Si/W ratios were presented in Figure 4.3. The peak intensities of catalysts were not different because the quantity of incorporated metal tungsten into the framework was in the vicinity, which was very

little as confirmed by ICP. The decrease of Si/W ratio or the increase in tungsten content of the samples affected the d-spacing of the (100) peak by decreasing from *ca.* 4.1-4.2 nm of the purely siliceous MCM-41 to 3.94 nm of W-MCM-41 with Si/W ratio in gel of 4, as shown in Table 4.1. The decrease of the interplanar spacing might be explained by the decrease of the wall thickness of W-MCM-41 sample on the basis of replacing longer Si-O bonds with shorter W-O bonds. Besides, the increasing in tungsten content of the samples caused the (100) diffraction peak broader and less intense. The change of the T-O-T bond angle due to the incorporation of tungsten in the framework structure results in a distortion of the long-range ordering of the hexagonal mesoporous structure and the disappearance of the (110) and (200) diffractions. This distortion is very significant when the Si/W ratio in gel of the starting mixture was lower to 4 as shown in Figure 4.3. Thus, the maximum content of tungsten that could be incorporated into the MCM-41 samples without destruction of the mesoporous structure is about 4.59% wt. In addition, the preparation of a gel mixture with Si/W < 4 resulted in an amorphous structure.

Table 4.1 The values of Bragg's angle and the corresponding d-spacing of W-MCM-41 samples synthesized from the gel with various Si/W ratios

Si/W molar ratio in gel	**d_{100} (Å)**	**Bragg's angle, 2θ (°)**
50	41.25	2.14
8	42.43	2.08
4	39.40	2.24

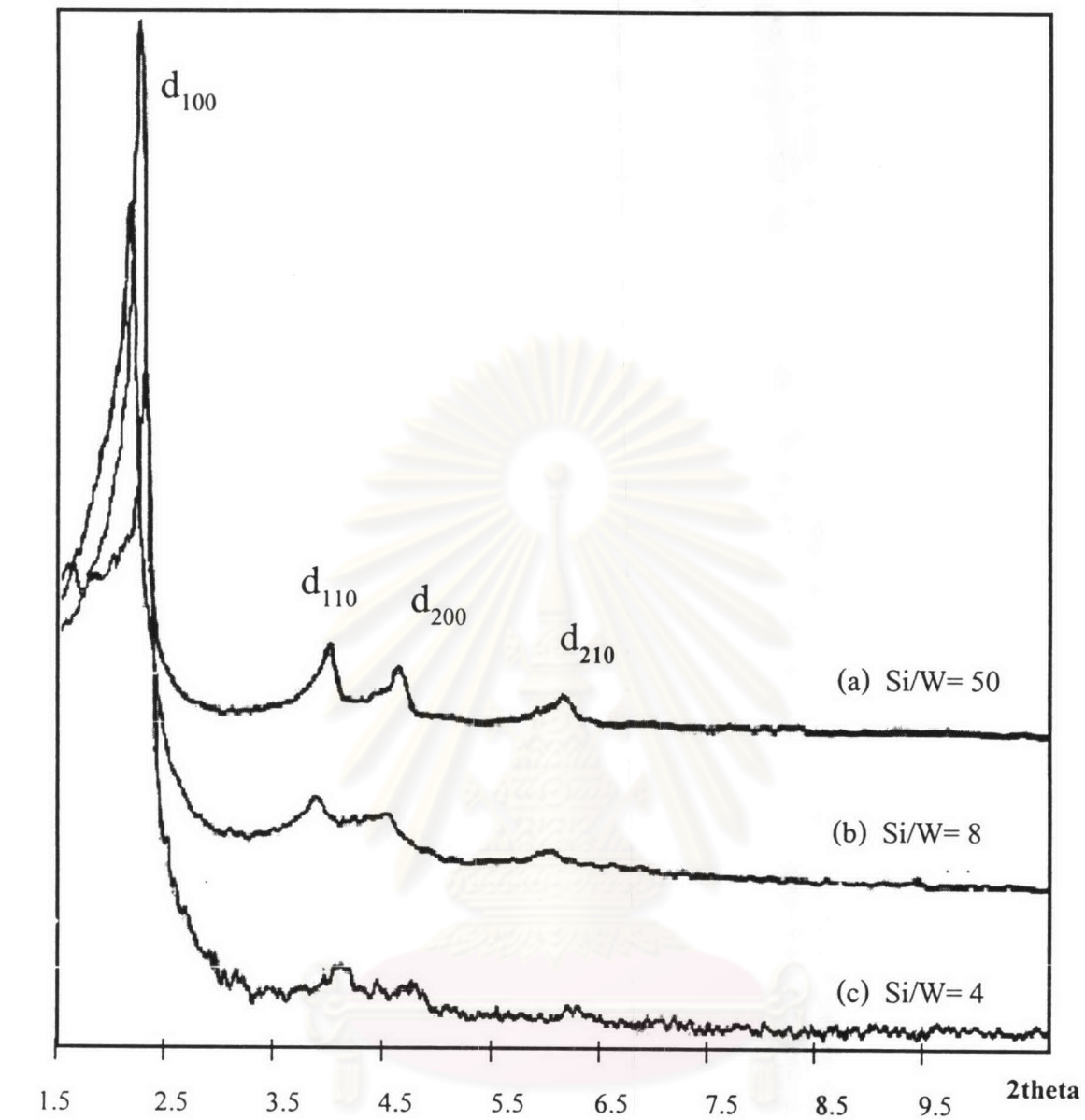

Figure 4.3 X-ray diffraction patterns of as-synthesized W-MCM-41 catalysts with various Si/W ratios in gel of (a) 50, (b) 8 and (c) 4.

(b) Catalyst Porosity

In order to evaluate the porosity of the materials, N_2 adsorption analysis was carried out. Figure 4.4 shows the N_2 adsorption-desorption isotherms of the W-MCM-41 samples. All samples exhibit a well-expressed hysteresis loop of type IV and have similar isotherms with an inflection around P/Po = 0.3, which is the characteristic behavior of mesopore materials.[66] However, as the Si/W ratio decreases, the hysteresis loop becomes broaden, resulting from the difficulty in formation of mesoporous structure when the tungsten content is high. Figure 4.5 shows a narrow pore size distribution of W-MCM-41, which indicated that W-MCM-41 synthesized has uniform structure.

BET specific surface area and pore size diameter of the W-MCM-41 catalysts were also obtained by the nitrogen physisorption method, and the data were summarized in Table 4.2. The specific surface area and the pore volume in the mesopores decrease with the increase in the tungsten content. These can be explained by the destruction of the pore structure of W-MCM-41 catalysts. The higher the tungsten content in the structure, the poorer the hexagonal crystalline materials obtained, which was in agreement with the XRD results.

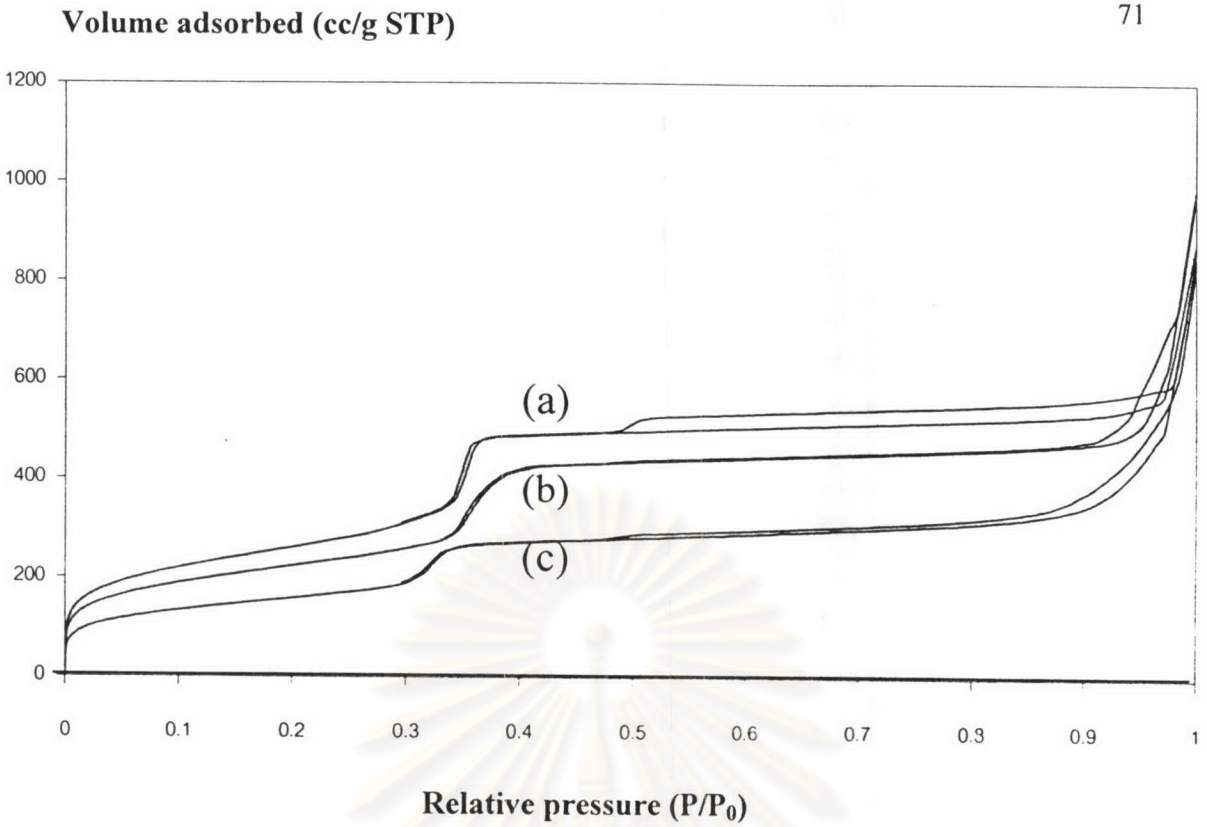

Figure 4.4 N_2 adsorption-desorption isotherm of W-MCM-41 with various Si/W ratios in gel of (a) 50, (b) 8 and (c) 4.

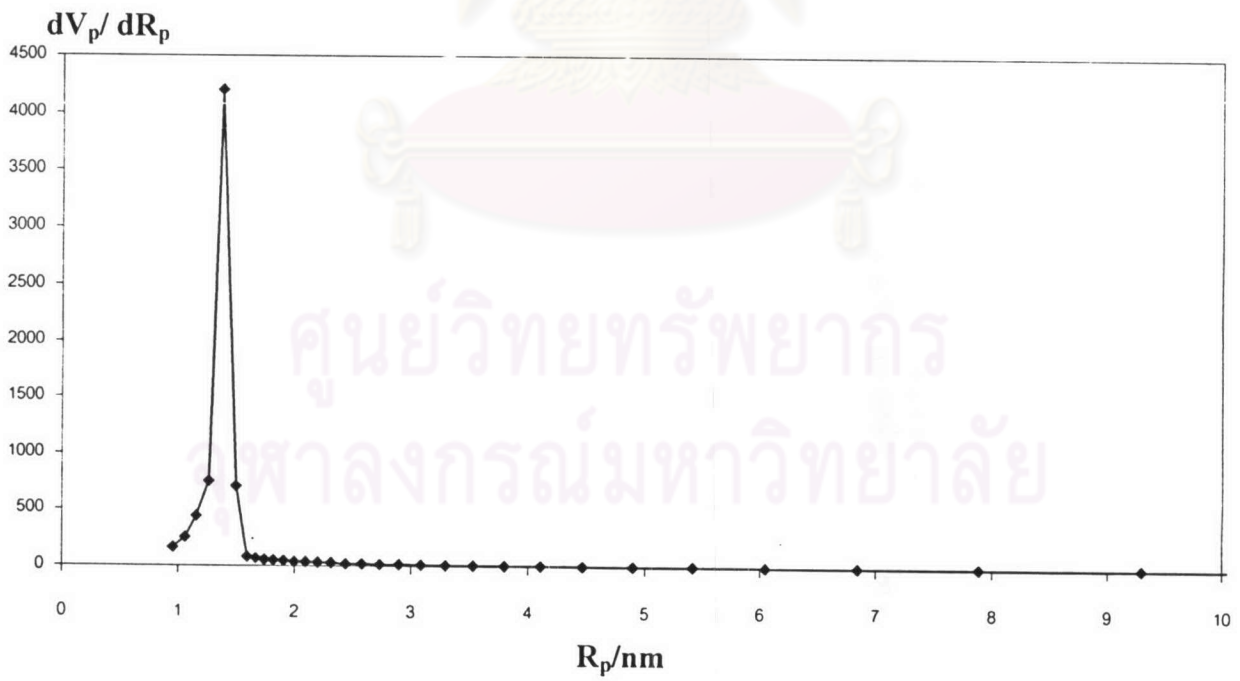

Figure 4.5 Pore-size distribution of W-MCM-41 with the Si/W ratio in gel of 50.

Table 4.2 The values of BET specific surface area and pore diameter of W-MCM-41 samples synthesized from the gel of various Si/W ratios

Si/W ratio in gel	BET specific surface area (m^2/g)	Pore diameter (Å)
120	936	28.6
100	1002	30.0
80	703	27.4
60	956	28.6
50	940	28.6
8	804	28.6
4	560	28.6

(c) ICP Analysis Results

In this work, W-MCM-41 samples with Si/W ratios > 50 in gel, which have almost no tungsten species did not have the interaction with the wall of MCM-41 in the step of mesostructure formation and they were released easily by washing with water. An attempt to incorporate tunsten into framework by overloading the excess amount of tungsten have been performed successfully in this study using ammonium tungstate as the tungsten source in basic condition. Tungsten content incorporated in W-MCM-41 samples was determined by ICP analysis after they were digested in HF and HCl solutions. The output data were calculated in terms of Si/W ratio and presented in Table 4.3. It has been observed that with increasing the tungsten content in gel, tungsten incorporated into the MCM-41 structure would be increased and the maximum tungsten content with Si/W in gel of 4 gave the Si/W in product of 84. In addition, the maximum of tungsten content corresponds to the XRD results.

Table 4.3 Analysis data of W-MCM-41 samples synthesized from the gel of various Si/W ratios

Si/W ratio in gel	Si/W ratio in product
120	2668
100	2014
80	1923
60	2592
50	1613
8	383
4	84

(d) FT-IR spectra

The FT-IR spectra of W-MCM-41 samples, shown in Figure 4.6, were performed upon the incorporation of W into the silica-based mesostructure. The vibration at ca. 960 cm^{-1} is attributed to the W-O-Si linkage. The lack of absorption bands at ca. 929, 880 and 774 cm^{-1} that would be attributed to the Keggin W-O stretching vibration[50] suggests the absence of Keggin units in the W-MCM-41 samples. However, in the FT-IR spectrum of the W-MCM-41 sample with the Si/W ratio in gel of 4, the vibrations at 929, 880 and 774 ascribed to the WO_6 group still remain unseen. The IR data indicates no formation of the WO_6 units outside the framework; however it cannot be taken as a reliable evidence for metal incorporation into pure siliceous MCM-41. The reason is that the region is very sensitive to any kind of metal-O vibration and it is still present a strong absorption band even in the pure silica MCM-41.

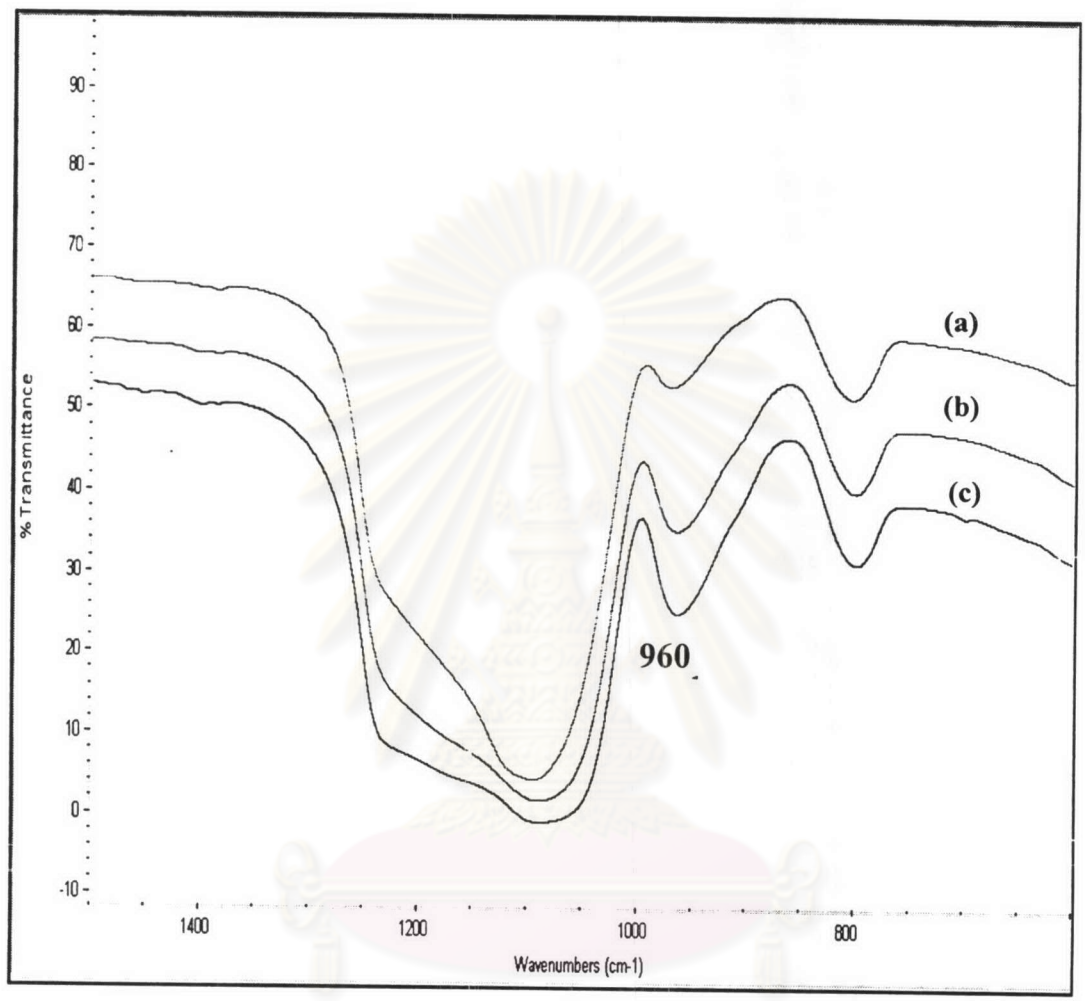

Figure 4.6 FT-IR spectra of W-MCM-41 with various Si/W ratios in gel of (a) 50, (b) 8 and (c) 4.

(e) Laser Raman Spectra

Laser Raman spectroscopy has been widely used to identify the condensed transition metal oxide phases in the characterization of various transition metal-containing composites. In Figure 4.7 showing the Laser Raman spectra of WO_3, pure silica-MCM-41 and W-MCM-41 with Si/W ratios of 50 and 4, it has been found that the Laser Raman spectra of W-MCM-41 samples resemble to those of pure silica MCM-41, as reported by Zhang[50], which indicates that tungsten atoms are isolated in the quasi-crystalline silica based frameworks. In addition, the Raman spectra of W-MCM-41 and pure silica MCM-41 in this study are shifted at ca. 400 cm^{-1} and more intense than the corresponding peaks reported by Zhang. This might be due to the differences in MCM-41 preparation methods. Besides, no scattering due to crystailine WO_3 particles[67] at 272, 325, 715 and 807 cm^{-1} is observed for the W-MCM-41 samples. This indicates that tungsten is incorporated into the MCM-41 framework. For the sample W-MCM-41 with Si/W in gel of 4, the less intense spectra at the Raman shift 802 cm^{-1} may be represented to the initial formation of tungstic oxide on the surface or it is the maximum Si/W ratio for the W-MCM-41 structure not being destroyed, as shown in Figure 4.8. These results are in agreement with XRD and DR UV-Vis results.

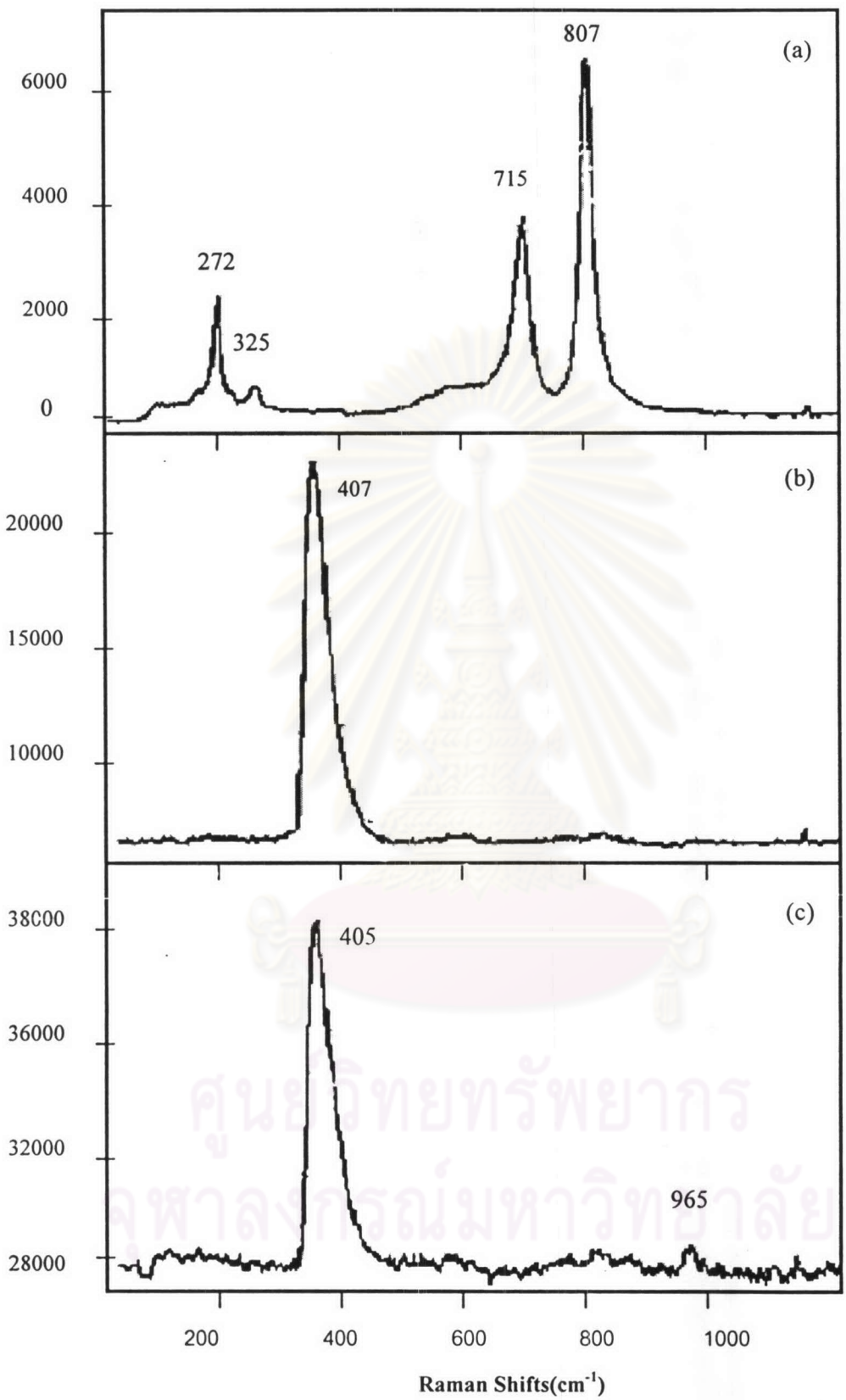

Figure 4.7 Laser Raman spectra of samples (a) WO_3, (b) Si-MCM-41 and (c) W-MCM-41 with the Si/W ratio in gel of 50.

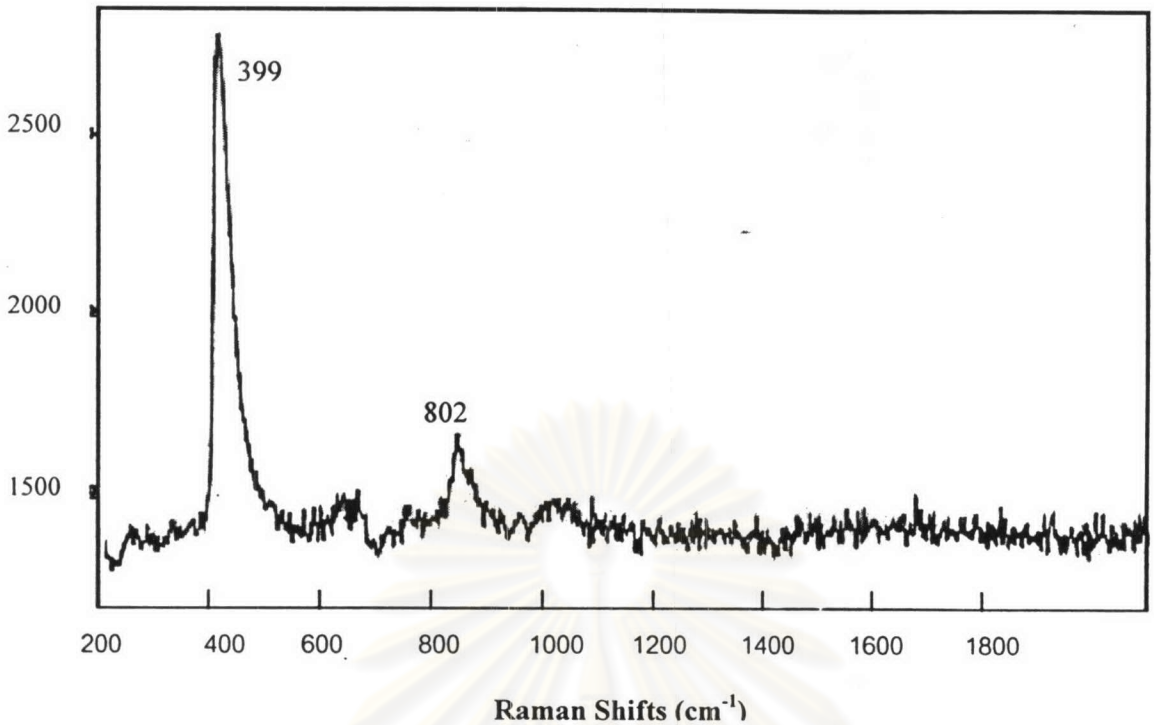

Figure 4.8 Laser Raman spectrum of W-MCM-41 with the Si/W ratio in gel of 4.

(f) DR-UV-Vis Spectra

Figure 4.9 shows the DR-UV-Vis spectra between 200 and 600 nm for the W-MCM-41 samples. Two major bands at 220 nm and 260 nm can be observed for all samples. Reference spectra,[68] belong to solid sodium tungstate (d) exclusively constituted of tetrahedral tungsten; ammonium metatungstate (e) and tungsten oxide (f) both mainly constituted of octahedral tungsten (tetrahedral species are also present as terminal tungsten atoms). By comparing the W-MCM-41 spectra with the reference spectra, it was concluded that the band at 220 nm could be assigned to the tetrahedral W(VI) species while the band at 260 nm could be assigned to the distorted tetrahedral W species. Besides, W-MCM-41 samples do not present the band at 375 nm which belongs to WO_3 crystallites. When the tungsten loading increases, the absorption band around 310 nm becomes broader. This indicates the subsequent formation of distorted tetrahedral tungsten species.

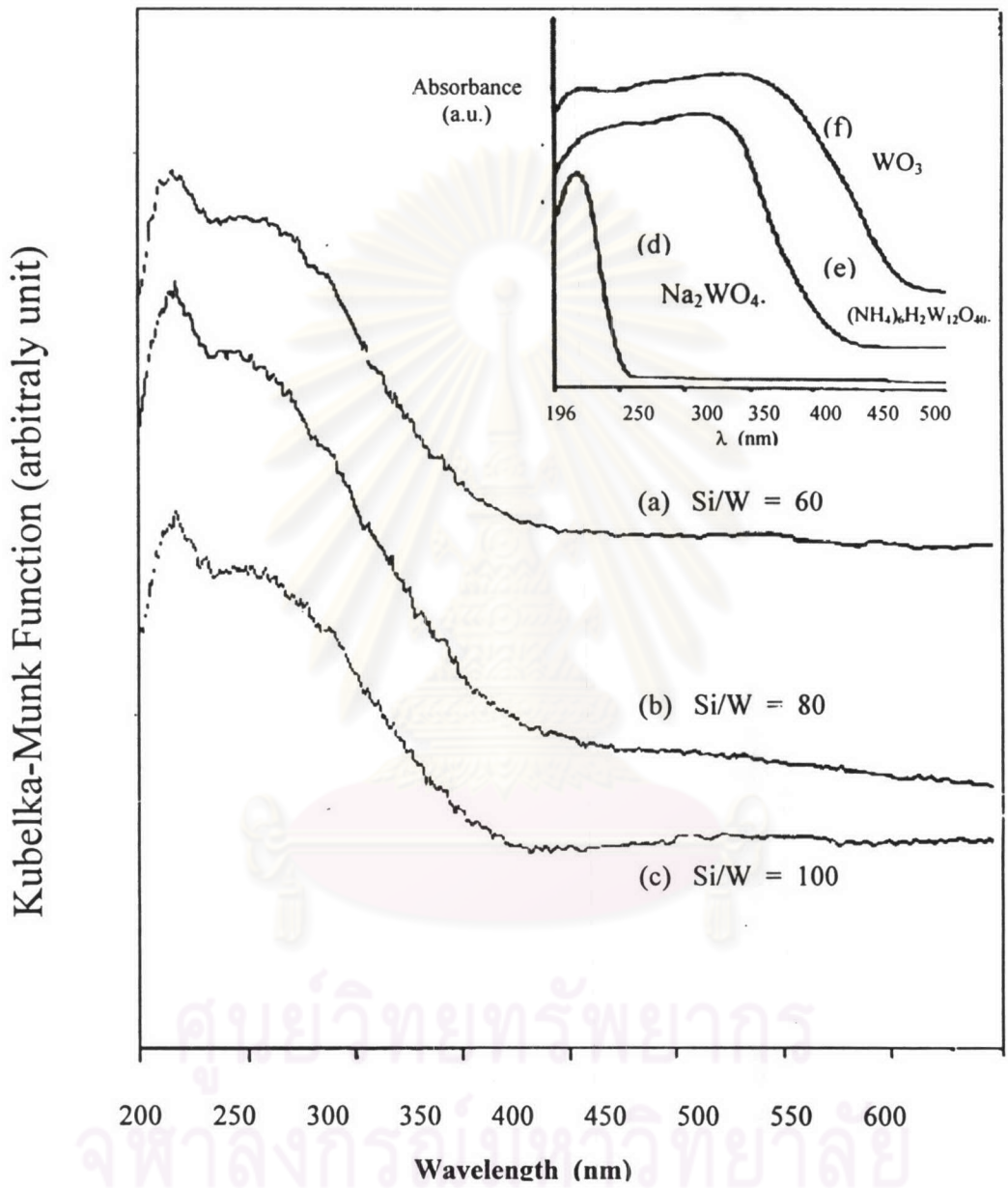

Figure 4.9 DR-UV-Vis spectra of calcined W-MCM-41 with various Si/W ratios in gel of (a) 60, (b) 80 and (c) 100 (d) Na_2WO_4 (e) $(NH_4)_6H_2W_{12}O_{40}$ (f) WO_3.

From the spectroscopic studies, it has been confirmed that all W-MCM-41 have some tungsten in tetrahedral coordination, as monotungstate species (WO_4^{2-} group) in the MCM-41 framework structure, Figure 4.10, and some tungsten, only in the high loading samples as distorted tetrahedral tungsten in extra framework.

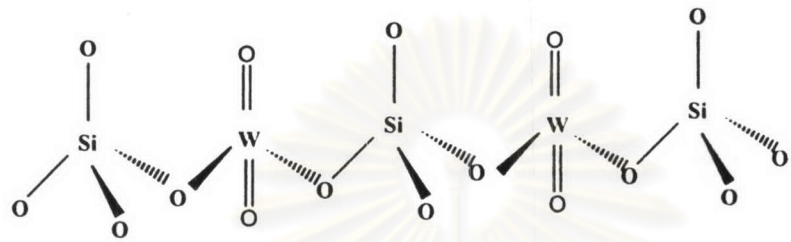

Figure 4.10 Model of the joining of the tetrahedral monomeric W species in the MCM-41 framework structure.

4.1.5 Effect of Template Removal

The template removal was achieved by calcination of the as-synthesized sample in air. Figture 4.11 shows the result of peak intensities of as-synthesized and calcined samples. The diffraction peaks become sharper and more intense upon calcination, that agree to other metal-containing MCM-41. From the liquid crystal mechanism of M41S formation, the as-synthesized MCM-41 sample with surfactant molecules most likely arranged in a micellar array. Upon calcination, the organic template was burnt off, leaving inorganic hollow in a hexagonal regular arrangement and resulted in the increasing in intensity of hexagonal characteristic peaks.[69]

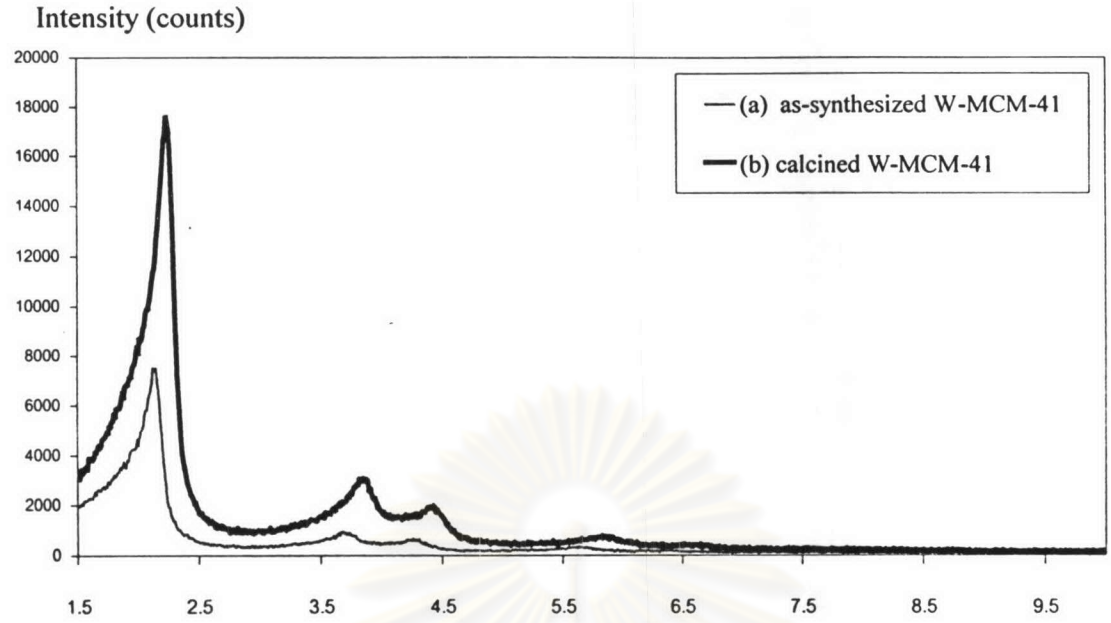

Figure 4.11 XRD patterns of MCM-41 with the Si/W in gel of 100, (a) before and (b) after calcination at 540°C for 6 hours.

4.2 Characterization of WO_3/MCM-41

(a) XRD Results

The XRD pattern of impregnated with WO_3 MCM-41 was shown in Figure 4.12. When compared with the Si-MCM-41 sample, the d_{100} peak was less intense and broaden because WO_3 on the MCM-41 surface has effect on the pore structure. Sodium tungstate, a tungsten source, coated on the mesophase was transformed to tungstic oxide after calcination at the temperature of 500°C. These condensed tungstic oxide on the surface might use oxygen atoms of the framework MCM-41 as supports, that cause the structure to collapse after impregnation. Besides, MCM-41 structure is itself not stable in aqueous solution.

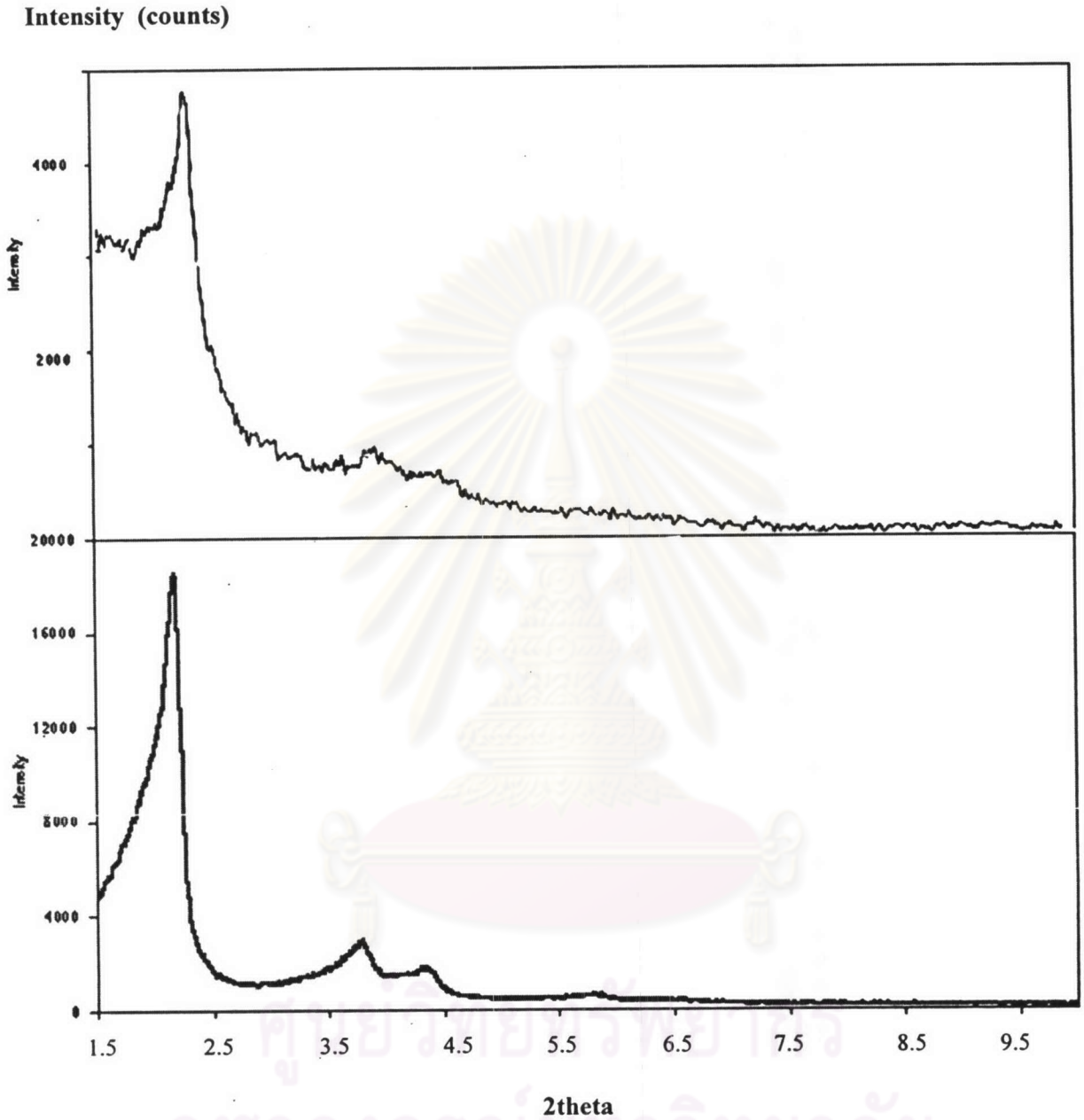

Figure 4.12 XRD patterns of (a) WO_3/MCM-41 with the Si/W ratio in product of 84 and (b) pure silica MCM-41 before impregnation.

(b) Specific Surface Area

The values of BET specific surface area of impregnated samples were 500-600 m^2/g, which less than the surface area of W-MCM-41 at the same Si/W ratio. This result is in accordance with Rana *et al.*[66] It was reported that the decrease in surface area for the impregnated molybdenum oxide on MCM-41 samples was attributed to the loss in crystallinity seen in the XRD patterns and the impregnated samples were covered by metal oxide species, confirmed by the band at 315 nm of DR-UV-Vis spectra.

Table 4.4 Nitrogen physisorption data of WO_3/MCM-41 samples

WO_3/MCM-41 (Si/W)	Specific surface area (m^2/g)	Pore diameter (Å)
1615	557.18	19
383	549.90	19
84	654.43	19

4.3 Catalytic Activities of W-MCM-41 and WO_3/MCM-41 Catalysts for Metathesis of 1-Hexene

4.3.1 Effect of Temperature on Catalytic Activities

The catalytic results for conversion of 1-hexene over W-MCM-41 (Si/W = 84) at various reaction temperatures are tabulated in Table 4.5 and Figure 4.14. With increasing reaction temperatures from 300 to 400 and 500°C, conversions of 1-hexene

increase from 88.31 to 93.98 and 98.49%, respectively. The conversion of 1-hexene to gaseous products is considerably predominant to liquid products at all temperatures. Formation of propylene is not significantly different at each temperature. Among gaseous products formation of butenes is favored at 300°C while formation of ethylene as well as methane is favored at high temperatures. Isomerization of 1-butene to its isomers is observed at 300°C and isobutene is found as the major product among isomeric butenes. At higher temperatures of 400 and 500°C, butenes can be readily converted to ethylene as the metathesis product in the presence of the tungsten-containing catalyst. Methane and coke are formed due to cracking of hydrocarbons at elevated temperature. It is noted that ethylene is not further converted to methane as found in other reactions over acid catalysts. The catalyst became gray after utilization at 300°C but black at higher temperatures. All turned to white again after regeneration at elevated temperature. By considering the highest selectivity to ethylene and the lowest selectivity to butenes, the reaction temperature of 500°C is preferred for further studies of variations in metathesis of 1-hexene.

Table 4.5 Catalytic activity of W-MCM-41 (Si/W = 84) in metathesis of 1-hexene at various temperatures, feed of 30.5% 1-hexene in nitrogen, the GHSV of 500 h^{-1}, time on stream of 30 min.

	Reaction Temperatures		
	300°C	400°C	500°C
Conversion of 1-hexene (%)	88.31	93.98	98.49
Yield of gas product (% wt)	70.80	69.52	68.40
Yield of liquid product (% wt)	11.62	2.34	1.99
Coke (% wt of catalyst)	11.23	18.20	18.57

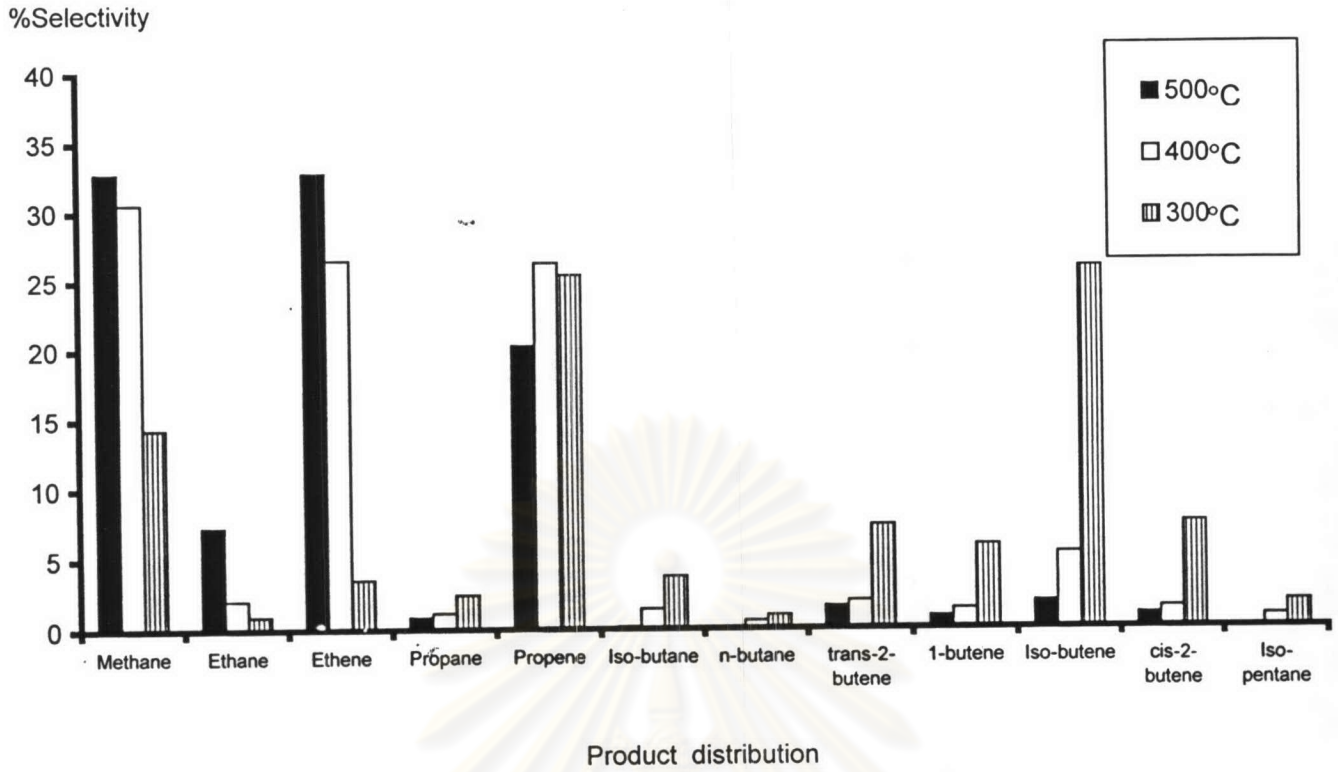

Figure 4.13 Product distribution in 1-hexene metathesis over W-MCM-41 (Si/W = 84) at various temperatures.

4.3.2 Catalytic Activity of W-MCM-41 with Various Si/W Ratios

The catalytic results for conversion of 1-hexene over W-MCM-41 catalysts with the Si/W ratio of 84, 383, and 1613 at the reaction temperature of 500°C are shown in Table 4.6 and Figure 4.14. All catalysts are highly active to conversion of 1-hexene and the major product is a mixture of methane, ethylene and propylene. Increasing the tungsten content resulting in lower Si/W ratio, conversions of 1-hexene increase from 90.74 to 94.30 and 98.49%, respectively. Liquid product amounts are reverse to the conversion extents. This implies that increasing the tungsten content in W-MCM-41 results in the greater number of active sites which can efficiently convert the liquid phase to gas. The highly dispersion of tungsten on the catalyst makes the infrastructure tungsten highly active for the metathesis reaction as well.

have a strong effect on type and amount of products. Selectivity to propylene increases in the order of Si/W in catalyst of 1613 > 84 > 383. The increase in selectivity to ethylene is in the reverse order: W-MCM-41 with the Si/W of 383 gives the best selectivity to ethylene along with the lowest selectivity to butenes. Besides, methane is formed in a significant amount for all cases while propane and butenes are rather scarce. Formation of coke on the used catalysts increases in amount when the ratios of Si/W increase. All catalysts become black after the single run and turn to white again after regenerated at elevated temperature.

Table 4.6 Catalytic activity of W-MCM-41 with various Si/W ratios in metathesis of 1-hexene at the temperature of 500°C, feed of 30.5% 1-hexene in nitrogen, the GHSV of 500 h^{-1}, time on stream of 30 min.

	W-MCM-41		
Si/W ratio in catalyst	1613	383	84
WO_3 content (% wt)	0.24	1.01	4.59
Conversion of 1-hexene (%)	90.74	94.30	98.49
Yield of gas product (% wt)	20.60	39.65	68.40
Yield of liquid product (% wt)	40.82	21.15	1.99
Coke (% wt of catalyst)	25.19	25.45	18.57

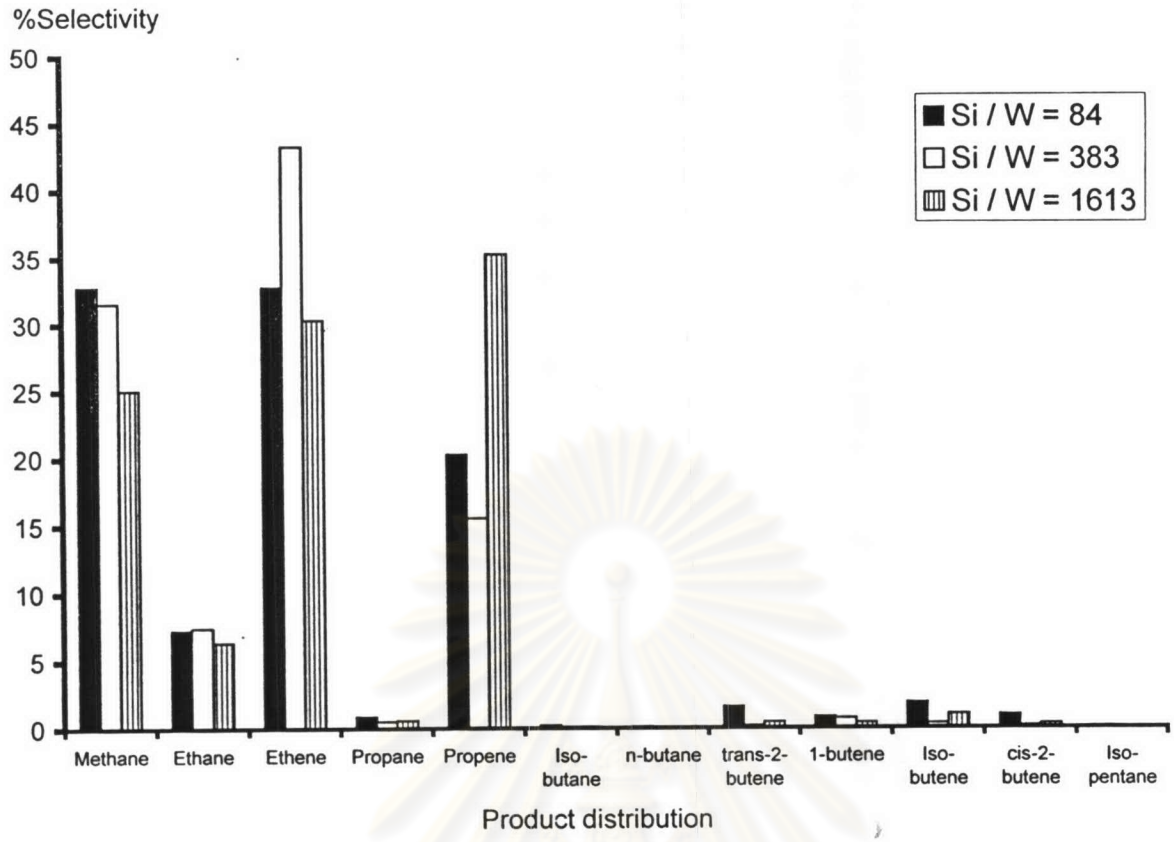

Figure 4.14 Product distribution in 1-hexene metathesis over W-MCM-41 with various Si/W ratios at 500°C.

4.3.3 Catalytic Activity of Impregnated WO_3/MCM-41

The results of metathesis reaction of 1-hexene over WO_3/MCM-41 with various Si/W ratios at 500°C are shown in Table 4.7 and Figure 4.15. Increasing tungsten content results in higher conversions of 1-hexene. This effect is significant when the WO_3 loading is below 1%. The conversion is not much affected by the tungsten content when the WO_3 loading is above 1%. This is because only the catalytic amount is necessary. The activities of WO_3/MCM-41 are much less than those of W-MCM-41 at all the same tungsten contents. This indicates that the tungsten containing MCM-41 prepared by direct synthesis method is more active than the catalyst prepared by the incipient wetness impregnation method.

Formation of liquid product by WO_3/MCM-41 does not get along with the tungsten contents in contrast to the catalysis over W-MCM-41. Coke formation on WO_3/MCM-41 decreases when increasing tungsten at low loading but decreases again at high loading of tungsten. Thus the results may indicate that the tungsten in WO_3/MCM-41 does not highly disperse in the structure of MCM-41. The excessive tungsten in WO_3/MCM-41 is not essentially active for metathesis of 1-hexene.

WO_3/MCM-41 at low loading favors the formation of isobutene is greater than all other hydrocarbons. The selectivity to isobutene decreases with the increase in tungsten content. Isobutene and its isomers further react to form ethylene and methane with increasing tungsten content. The behavior of WO_3/MCM-41 for 1-hexene conversion at 500°C at low loading of tungsten is similar to that of W-MCM-41 at lower temperature.

These results show that the tungsten-containing catalysts have different activities in metathesis of 1-hexene depending on the methods of preparation. Direct synthesis of W-MCM-41 results in highly dispersion of the tungsten active sites better than incipient wetness method of impregnation of WO_3 on MCM-41. Besides, the interaction of tungstate salt with the MCM-41 material during the course of preparation of the impregnated WO_3/MCM-41catalysts causes the partially destroyed MCM-41 structure. This affects the decrease of surface area and activity of the supported tungsten catalyst. The extremely high activity and selectivity of W-MCM-41 compared to tungsten supported catalysts can be promoted by the unique high surface area of uniform pore-system W-MCM-41 over others. While the species of polytungstates with W(VI) and octahedral WO_3 crystallites are formed in impregnated tungsten catalysts,[68] the isolated tetrahedral WO_4 and/or penta-coordinate $O=WO_4$ species in which W atoms are coordinatively unsaturated, are formed in the W-MCM-41 catalyst. The framework tungsten species can readily form active metal carbene which is required for the olefin metathesis. The catalysis results are in agreement with the XRD and DR-UV-VIS data.

Table 4.7 Catalytic activity of impregnated WO_3/MCM-41 with various Si/W ratios in metathesis of 1-hexene at the temperature of 500°C, feed of 30.5% 1-hexene in nitrogen, the GHSV of 500 h^{-1}, time on stream of 30 min.

	WO_3/MCM-41		
Si/W ratio in catalyst	1613	383	84
WO_3 content (% wt)	0.24	1.01	4.59
Conversion of 1-hexene (%)	13.15	58.73	61.28
Yield of gas product (% wt)	16.72	26.12	43.59
Yield of liquid product (% wt)	28.23	33.07	6.23
Coke (% wt of catalyst)	30.73	24.51	31.89

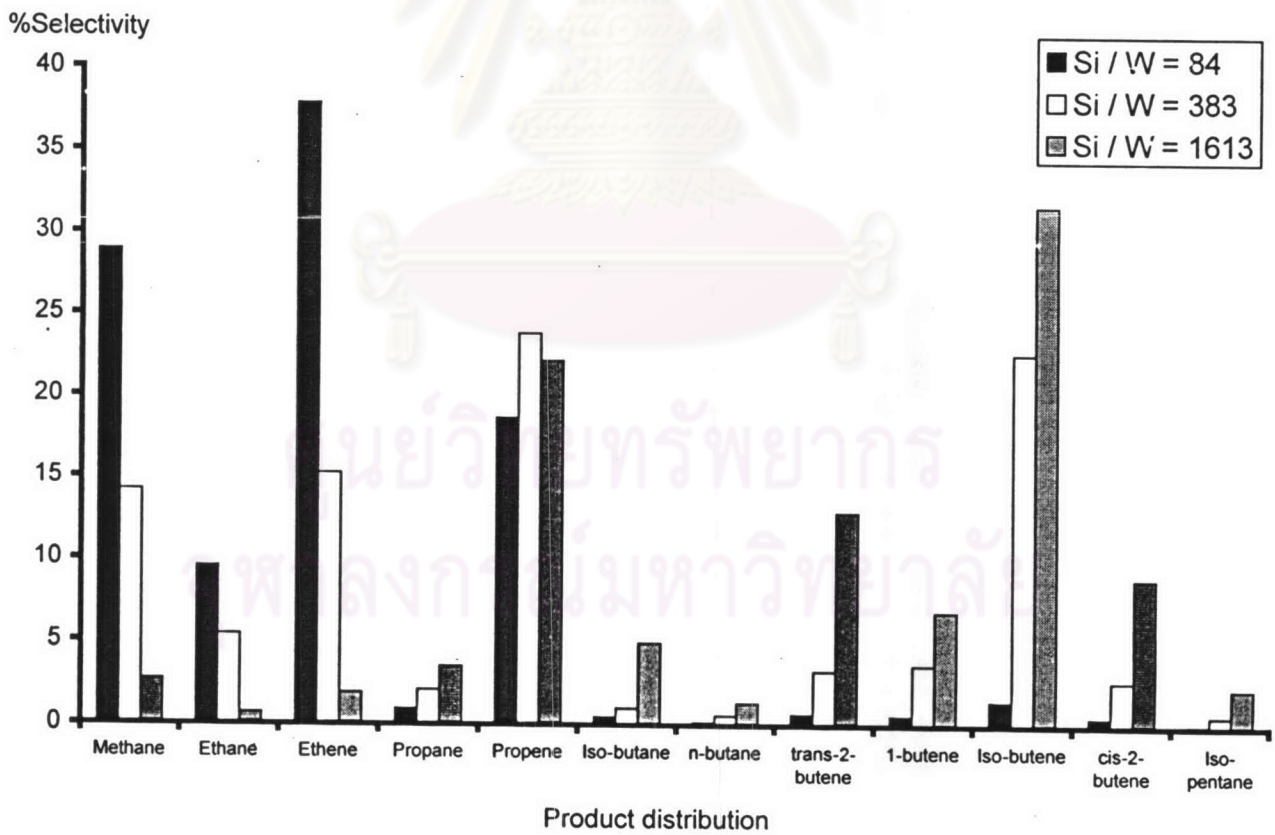

Figure 4.15 Product distribution in 1-hexene metathesis over impregnated WO_3/MCM-41 with various Si/W ratios at 500°C.